

# Homogeneous Nucleation and Fractionated Crystallization in Block Copolymers<sup>†</sup>

A. J. Müller,<sup>\*,‡</sup> V. Balsamo,<sup>‡</sup> M. L. Arnal,<sup>‡</sup> T. Jakob,<sup>§</sup> H. Schmalz,<sup>§</sup> and V. Abetz<sup>§</sup>

Grupo de Polimeros USB, Departamento de Ciencia de los Materiales, Universidad Simón Bolívar, Apartado 89000, Caracas 1080-A, Venezuela, and Makromolekulare Chemie II, Universität Bayreuth, 95440 Bayreuth, Germany

Received November 19, 2001; Revised Manuscript Received February 4, 2002

**ABSTRACT:** The confinement of crystallizable blocks within AB or ABC microphase-separated block copolymers in the nanoscopic scale can be tailored by adequate choice of composition, molecular weight, and chemical structure. In this work we have examined the crystallization behavior of a series of AB and ABC block copolymers incorporating one or two of the following crystallizable blocks: polyethylene, poly( $\epsilon$ -caprolactone), and poly(ethylene oxide). The density of confined microdomain structures (MD) within block copolymers of specific compositions, in cases where the MD are dispersed as spheres, cylinders, or any other isolated morphology, is much higher than the number of heterogeneities available in each crystallizable block. Therefore, fractionated crystallization takes place with one or several crystallization steps at decreasing temperatures. In specific cases, the clear observation of exclusive crystallization from homogeneous nuclei was obtained. The results show that, regardless of the specific morphological features of the MD, it is their vast number as compared to the number of heterogeneities present in the system that determines the fractionated character of the crystallization or in extreme cases homogeneous nucleation. The self-nucleation behavior was also found to depend on the composition of the copolymers. When the crystallizable block is confined into spheres or cylinders and exhibits homogeneous nucleation, the self-nucleation domain disappears. This is a direct consequence of the extremely high density of microdomain structures that need to be self-seeded (on the order of  $10^{15}$ – $10^{16}/\text{cm}^3$ ). Therefore, to increase the density of self-nuclei, the self-nucleation temperature has to be decreased to values so low that extensive partial melting is achieved, and some of the unmelted crystal fragments can be annealed, in some cases even before self-nucleation takes place.

## Introduction

The primary nucleation process in polymers usually occurs by one of the following: heterogeneous nucleation, homogeneous nucleation, and self-nucleation. The nucleation of semicrystalline polymers in the bulk usually occurs on existing heterogeneities (catalyst debris, impurities, and other types of heterogeneities sometimes of unknown nature). Homogeneous nucleation is rarely observed. However, if the bulk polymer is subdivided into isolated regions (most likely droplets in an immiscible matrix, like in immiscible blends or in microphase-separated domains like in block copolymers) whose number is of the same order of magnitude or greater than the number of usually active heterogeneities, a fractionated crystallization phenomenon will develop.

Let us consider a finely dispersed polymer in the form of droplets that is being cooled from the melt in a differential scanning calorimeter (DSC); it is highly probable that a series of crystallization exotherms are observed which can be interpreted as the crystallization of different groups of droplets at specific and independent supercoolings<sup>1,2</sup> since the original polymer in the bulk contains different types of heterogeneities. The droplets that contain the heterogeneities usually active at low supercoolings in the bulk polymer will crystallize at identical temperatures to that polymer in the bulk. Those droplets that contain other types of less efficient

heterogeneities will nucleate at a larger supercooling that is necessary for those heterogeneities to become active. Finally, those droplets that do not contain any heterogeneities will be able to nucleate homogeneously (if the interphase does not affect the nucleation process) at the largest supercooling, since a large supercooling is usually needed in order to generate homogeneous nuclei.

The homogeneous nucleation phenomena were first studied by droplet crystallization experiments performed in metals, alkanes, and polymers when dispersed in inert low molecular weight media.<sup>1–13</sup> Nevertheless, some authors found that the maximum supercooling needed for the crystallization of a certain droplet population was dependent on the superficial characteristics of the droplets. Both the crystallization of polymer droplets in inert low molecular weight media and in high molecular weight polymer matrices share the same limitations from the point of view of being susceptible to surface nucleation phenomena.<sup>3–13</sup> In the case of block copolymers, several factors contribute to make them an ideal system to study homogeneous nucleation: The purity involved in the synthesis, the size of the microdomain structures (MD) which can easily reach the nanoscopic scale, and the presence of interphases in strongly segregated systems which could lead to less interference from interphase nucleation than the interphase between disperse droplets and the matrix in immiscible blends. Nevertheless, this last possibility is difficult to rule out.

Encountering homogeneous nucleation in dispersed droplets can be difficult when the dispersion is on the micron scale. Since mixing immiscible two-phase systems has a limit in the particle size that can be achieved

<sup>†</sup> This work is dedicated to the memory of our friend and colleague Prof. Reimund Stadler.

<sup>\*</sup> To whom correspondence should be addressed.

<sup>‡</sup> Universidad Simón Bolívar.

<sup>§</sup> Universität Bayreuth.

**Table 1. Peak Crystallization Temperatures of AB and ABC Block Copolymers and Selected Homopolymers<sup>a,b</sup>**

sample	$T_c$ (I), °C	$T_c$ (I), °C	$T_c$ (II), °C	sample	$T_c$ (I), °C	$T_c$ (I), °C	$T_c$ (II), °C
PEO <sup>1</sup>		21		PE		PCL	PCL
PEO <sup>100</sup>		43		S <sub>27</sub> C <sub>73</sub> <sup>81</sup>		36.5	-39.8
PCL <sup>32</sup>		33.5		S <sub>62</sub> B <sub>27</sub> C <sub>11</sub> <sup>62</sup>		20.4	-45.1
PE <sup>19</sup> (2.6) <sup>a</sup>		73.4		S <sub>62</sub> E <sub>27</sub> C <sub>11</sub> <sup>62</sup> (3.8) <sup>a</sup>	71.5	10.1	
				S <sub>37</sub> B <sub>52</sub> C <sub>11</sub> <sup>96</sup>		6.4	-48.4
B <sub>17</sub> I <sub>57</sub> EO <sub>26</sub> <sup>130</sup>		15	-21	S <sub>37</sub> E <sub>52</sub> C <sub>11</sub> <sup>96</sup> (4.1) <sup>a</sup>		19.0	
B <sub>11</sub> I <sub>70</sub> EO <sub>19</sub> <sup>120</sup>			-23	S <sub>50</sub> B <sub>28</sub> C <sub>22</sub> <sup>97</sup>	75.4	10.3	-46.0
B <sub>24</sub> I <sub>56</sub> EO <sub>20</sub> <sup>67</sup>			-25	S <sub>50</sub> E <sub>28</sub> C <sub>22</sub> <sup>97</sup> (2.6) <sup>a</sup>	71.6	14.6	
E <sub>11</sub> EP <sub>71</sub> EO <sub>18</sub> <sup>124</sup> (6.4) <sup>a</sup>	PE	PEO	PEO	S <sub>26</sub> B <sub>36</sub> C <sub>38</sub> <sup>110</sup>		36.0	-40.8
original	52	22	-22	S <sub>26</sub> E <sub>36</sub> C <sub>38</sub> <sup>110</sup> (4.1) <sup>a</sup>	72.1	25.8	14.2
purified	51		-23	S <sub>20</sub> B <sub>41</sub> C <sub>39</sub> <sup>132</sup>		16.7	-43.7
E <sub>24</sub> EP <sub>57</sub> EO <sub>19</sub> <sup>69</sup> (5.8) <sup>a</sup>	PE	PEO	PEO	S <sub>20</sub> E <sub>41</sub> C <sub>39</sub> <sup>132</sup> (3.8) <sup>a</sup>	79.8	8.8	
original	69	20	-22	S <sub>37</sub> B <sub>11</sub> C <sub>52</sub> <sup>79</sup>		28.3	
purified	68		-27	S <sub>37</sub> E <sub>11</sub> C <sub>52</sub> <sup>79</sup> (5.6) <sup>a</sup>	45.0	27.0	-5.0
S <sub>81</sub> EO <sub>19</sub> <sup>18.5</sup>			-40	S <sub>23</sub> B <sub>21</sub> C <sub>56</sub> <sup>103</sup>		31.2	-39.6
S <sub>39</sub> EO <sub>61</sub> <sup>46</sup>		39		S <sub>23</sub> E <sub>21</sub> C <sub>56</sub> <sup>103</sup> (4.4) <sup>a</sup>	53.3	24.1	-3.3

<sup>a</sup> Numbers in parentheses indicate the content in mol % of ethyl branches in PE chains. <sup>b</sup> B = polybutadiene, I = polyisoprene, EO = poly(ethylene oxide), C = polycaprolactone, E = polyethylene, EP = poly(ethylene-co-propylene), S = polystyrene.

(usually the minimum being around 0.3–0.1  $\mu\text{m}$ , but with a wide distribution of particle size where many particles are usually on the order of 1  $\mu\text{m}$ ), this means that also the particle density has a limit that will probably be around  $10^{11}$ – $10^{12}$  particles/cm<sup>3</sup>. A polymer like high-density polyethylene (HDPE) has around  $10^9$  highly active heterogeneous nuclei/cm<sup>3</sup> in the bulk (this number does not include other type of less active heterogeneities that can possibly cause nucleation at larger supercoolings), so it may be difficult to get a large enough population of dispersed droplets that are heterogeneity free by blending with an immiscible component.<sup>14</sup> In a previous work, several PS/HDPE (polystyrene/HDPE), PS/LLDPE (linear low-density polyethylene), and PS/ULDPE (ultralow-density polyethylene) blends were prepared in a composition range where atactic polystyrene (PS) was always the matrix component.<sup>14</sup> All the types of polyethylenes employed, when dispersed into droplets, exhibited fractionated crystallization exotherms in the temperature range between 67 and 70 °C. These low crystallization temperatures are probably closer to the homogeneous nucleation temperature of linear polyethylene than any previously reported value for microns size droplets, since they occur at higher supercoolings.<sup>3,13</sup> The higher values of crystallization temperatures previously reported could be explained by the crystallization from heterogeneous nuclei of relatively low nucleation efficiency or by a weak nucleation capacity of the droplets interface. Recently, Loo et al.<sup>15</sup> have studied the crystallization of the polyethylene block within a E/SEB diblock copolymer constituted by hydrogenated polybutadiene (14.3 wt % E) and an amorphous random terpolymer of styrene-ethylene-butene (SEB). The PE block crystallized within 25 nm spherical mesophases, and most spheres were homogeneously nucleated since the number of MD was  $2 \times 10^{16}$  spheres/cm<sup>3</sup>. It is interesting to note that the authors also found crystallization temperatures between 66 and 69 °C for the PE block, which could be somewhat similar to a LLDPE in view of its branch content.

In the case of isotactic polypropylene (iPP), its intrinsic nucleation density is much lower since it contains only of the order of  $10^6$  heterogeneities/cm<sup>3</sup>; therefore, fractionated crystallization is relatively easy to obtain.<sup>2,16–19</sup> Arnal et al.<sup>19</sup> were able, through the use of a suitable compatibilizer, to produce fine dispersions of iPP in PS matrices. When a sufficient amount of a

compatibilizer was used to obtain very small particle sizes and more homogeneous dispersions, the iPP crystallized exclusively at a low-temperature exotherm that exhibited an onset at 51 °C and peaked at 46 °C. It was postulated that such crystallization was the result of homogeneously nucleated crystals forming in the approximately 1.5  $\mu\text{m}$  size droplets produced (the number of particles was  $1.3 \times 10^{11}$  droplets/cm<sup>3</sup>). Wide-angle X-ray diffraction measurements indicated that the iPP both in the bulk and in dispersed droplets crystallized in the monoclinic  $\alpha$ -phase; this evidence may rule out the possibility that the crystallization observed at 46 °C is due to the formation of another crystal modification or a mesomorphic phase.<sup>19</sup> Therefore, such an exclusive low-temperature exotherm may represent the dynamic crystallization during cooling of iPP heterogeneity free droplets that nucleate homogeneously at temperatures close to 51 °C.

The finding of extremely large supercoolings attributable to crystallization starting from homogeneous nuclei in diblock copolymers minor phase components dates back to 1969<sup>1,20</sup> and has been the subject of recent attention.<sup>15,21–24</sup> In the case of ABC triblock copolymers, only a few works have reported fractionated crystallization of one crystallizable component.<sup>25,26</sup> We have recently presented results on ABC triblock copolymer systems where two crystallizable components can exhibit fractionated crystallization depending on the composition.<sup>27–29</sup>

In this work we examine the fractionated crystallization and homogeneous nucleation in a wide selection of AB diblock and ABC triblocks containing one or two crystallizable components that can experience fractionated crystallization. The wide selection of copolymers allows confinement of crystallizable blocks to be studied in very different types of microdomain morphologies like cylinders, spheres, undulated layers, rings, and lamellae. Nevertheless, our results show that, regardless of the specific morphological features of the MD, it is their vast number as compared to the heterogeneities present in the system that determine the fractionated character of the crystallization or in extreme cases exclusive homogeneous nucleation. The effect of confinement is also found to greatly affect the self-nucleation behavior of the crystallizable blocks within AB and ABC copolymers.

## Experimental Section

Table 1 lists the materials employed in this work where the subscripts indicate the amount of each component in wt % and the superscripts the average number molecular weight in kg/mol. The PEO samples were supplied by Polysciences. The rest of the polymers and copolymers were synthesized employing sequential living anionic polymerization and hydrogenation techniques described previously.<sup>26,30–32</sup> Polydispersity was less than 1.2 for most samples.

All DSC runs were performed in a Pyris 1 from Perkin-Elmer under an ultrapure nitrogen atmosphere calibrated with cyclohexane and indium. AB and ABC triblock copolymer samples of powders obtained after precipitation in 2-propanol were used. This means that all DSC results were obtained in as-synthesized samples with no prior annealing treatment.

The self-nucleation technique designed by Fillon et al.<sup>33</sup> was employed in order to ascertain the self-nucleation domains for the homopolymers and copolymers; details of experimental procedure can be found in previous works.<sup>2,14</sup> Samples are first heated to a high enough temperature in order to erase thermal history. (A temperature of at least 25 °C higher than the melting peak of the highest melting peak temperature in the sample was used, typically 140 °C for 3 min.) Then they are cooled at 10 °C/min down to –100 °C to provide them with a “standard” thermal history.<sup>33</sup> Subsequently, they are heated to a temperature denoted  $T_s$  (or self-nucleation temperature) and isothermally kept there for a constant time of 5 min. After treatment at  $T_s$ , the sample is cooled to –100 °C and heated again at 10 °C/min until full melting occurs. Depending on  $T_s$ , the sample can be in one of three general domains: In domain I the sample is completely molten; in domain II the sample is self-nucleated since  $T_s$  is high enough to melt almost all crystals, but small fragments that can act as self-nuclei remain and the nucleation density can be enormously increased by small changes in  $T_s$ ; in domain III the sample is partially molten so that self-nucleation and annealing of unmelted crystals will take place at  $T_s$ .<sup>33</sup>

Transmission electron microscopy (TEM) observations were performed in a Zeiss CEM 902 electron microscope at 80 kV. Films of 1 mm thickness were casted from chloroform solutions at room temperature. The SBC films were annealed at 140 °C (a temperature below the order–disorder transition that was measured rheologically and was located at  $T > 170$  °C) for 4 h before cooling them to an isothermal crystallization temperature (that was varied depending on the specific copolymer, but was in the range 43–48 °C), where they were kept for 12 h. Films of SEC block copolymers were annealed at 160 °C and isothermally crystallized at 75 °C for the same time as SBC copolymers; the order–disorder transition temperature for SEC polymers is well above 200 °C. After the thermal treatment, thin sections (ranging between 40 and 60 nm thick) were cut with the help of a Reichert-Jung Ultramicrotome equipped with a diamond knife. These were later stained with OsO<sub>4</sub> or RuO<sub>4</sub> depending on the sample characteristics.

## Results and Discussion

The general behavior of fractionated crystallization of confined crystallizable blocks within AB and ABC copolymers will be presented first along with the effects of impurities provided by hydrogenation catalysts in some of the samples. A wide selection of compositions will be used and will provide a rich morphological spectrum. Finally, the changes in self-nucleation behavior experienced by the crystallizable blocks when they are confined in microdomain structures will be analyzed.

**Fractionated Crystallization in PS-*b*-PEO Diblock Copolymers.** Figure 1 presents the typical crystallization and melting behavior of PS-*b*-PEO diblock copolymers where both composition and molecular weight have been varied. The reason behind the 30 °C difference in melting point between the two samples is due

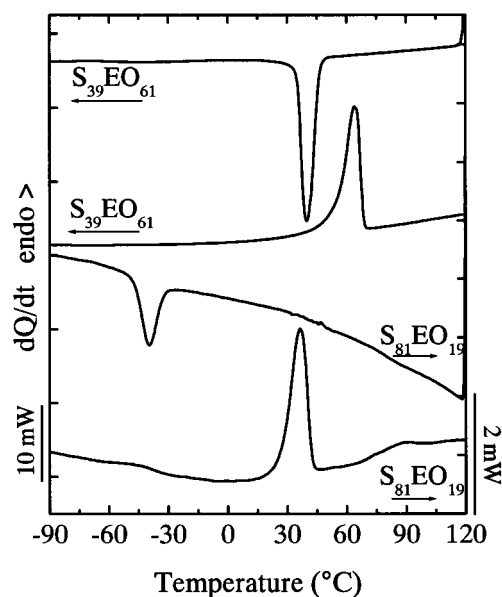


**Figure 1.** Cooling and heating DSC scans (10 °C/min) for PS-*b*-PEO diblock copolymers.

to differences in molecular weight of the PEO block. As a reference, we have measured PEO homopolymers using identical conditions to those of Figure 1, and we have found that the peak melting temperature of PEO changed from 40 to 65 °C when the molecular weight was increased from 1 to 100 kg/mol.

The cooling scan of the S<sub>39</sub>EO<sub>61</sub><sup>46</sup> diblock copolymer exhibits a sharp crystallization exotherm at 37 °C, corresponding to the crystallization of the PEO block after heterogeneous nucleation. This is the expected behavior for a copolymer where the major component is PEO. However, when PEO is the minor component as in the S<sub>81</sub>EO<sub>19</sub><sup>18.5</sup> diblock copolymer, the PEO phase will typically crystallize from a phase segregated melt into confined microphases, which in this case must correspond to PEO cylinders in view of the composition.<sup>22,34</sup> The order–disorder transition is expected at temperatures of 160 °C for this type of copolymer,<sup>22</sup> and the crystallization of the PEO from this strongly segregated melt occurs after vitrification of the PS matrix. (The  $T_g$  of the PS phase can be clearly seen after the PEO fusion in Figure 1 for this copolymer.) As a result of the much higher density of cylinders than heterogeneities, the crystallization occurs at extremely low temperatures, starting at –30 °C, going through an exothermic peak at –40 °C, and finally ending at around –50 °C. This low-temperature crystallization indicates that apparently all of the PEO block is being homogeneously nucleated, since the  $T_g$  of the PEO block was determined by DSC to be around –58 °C, and therefore this polymer is attaining the maximum possible supercooling before crystallizing (i.e., a characteristic of homogeneously nucleated crystallization). These results corroborate previous findings in the literature for this type of copolymer.<sup>20–22</sup>

Since the crystallization occurs just before vitrification of PEO, it is expected that the amount of crystals formed is probably going to be much smaller for the confined PEO block within the PS matrix in S<sub>81</sub>EO<sub>19</sub><sup>18.5</sup> than for the PEO block in S<sub>39</sub>EO<sub>61</sub><sup>46</sup>. However, it is still surprising to find out that upon crystallization the corresponding latent heats are –83 J/g for S<sub>39</sub>EO<sub>61</sub><sup>46</sup> and only –6 J/g for S<sub>81</sub>EO<sub>19</sub><sup>18.5</sup> (the enthalpies of crystallization are



of course normalized to the amount of PEO within the copolymers), a fact that explains the use of very different scales for each block copolymer DSC curve in Figure 1. The rather small number of crystals formed within the PEO cylinders must also be thinner and more defective, when compared to those formed in the heterogeneously nucleated homopolymer, in view of their extremely low crystallization temperature. This probably accounts for the cold crystallization behavior that can be seen in the heating scan of  $S_{81}EO_{19}^{18.5}$  in Figure 1. At least  $-9$  J/g was detected as the heat of cold crystallization, which added to the  $-6$  J/g evolved during cooling closes the heat balance after melting, since the fusion enthalpy measured was 15 J/g.

In the above analysis, the observation of exclusive crystallization from homogeneous nuclei for confined PEO can be explained since the number of heterogeneous nuclei present in PEO could be comparable to that of iPP since they both form rather large spherulites of  $50\text{--}100\text{ }\mu\text{m}$  in size or larger in the PEO case depending on crystallization conditions. So, a nucleation density of  $10^6$  nuclei/cm<sup>3</sup> or even much lower is expected for PEO, and a much larger number of PEO cylinders within a PS matrix would be expected for a diblock copolymer of  $S_{81}EO_{19}^{18.5}$ . (A minimum of  $10^{14}$  cylinders/cm<sup>3</sup> could be present for cylinders in the nanometer range; see below concrete examples in the case of block copolymers containing poly( $\epsilon$ -caprolactone), PCL.)

In a recent work by Chen et al.,<sup>22</sup> PEO-*b*-PB/PB blends (PB = polybutadiene) were prepared in order to provoke increasing confinement of the PEO block as the amount of PB was increased. The authors found that peak crystallization temperatures apparently depended on the volume of dispersed PEO, so that when it was confined into cylinders, the crystallization peak temperature occurred at approximately  $-25$  °C, and when it was confined into spheres, it decreased further to  $-34$  °C. The authors argued that the PEO was crystallizing from homogeneous nuclei in both cases and that the probability of homogeneous nucleation was proportional to the volume of the microphase-separated domain. This interpretation requires that the microdomain structures (MD) are so small that they interfere with the homogeneous nucleation of polymer chains. This can only happen when the confinement volume is of the same order of magnitude or smaller than the size of the critical nucleus. However, a recent work by Huang et al.<sup>35</sup> has reported that when isothermal crystallization of PEO confined cylinders (within a PS matrix) is carried out at temperatures between  $-50$  and  $-30$  °C, a random orientation of the crystals with respect to the cylinder surfaces is encountered. The authors argue that the nucleation density is so high that little crystal growth is needed to complete crystallization in view of the deep supercooling, and therefore the PEO crystals produced are too small to "feel" the two-dimensional cylindrical confinement within the 13.7 nm diameter cylinders. At crystallization temperatures greater than  $-30$  °C, alignment of crystallites was produced. These results back up our interpretation given above about the origin of fractionated crystallization in the sense that it may not have to be the confinement in itself what is causing the homogeneous nucleation in crystallizable blocks, but instead a consequence of confinement, i.e., the lack of a high enough number of heterogeneities.

#### Fractionated Crystallization of PE-*b*-PEP-*b*-PEO Triblock Copolymers and the Effect of Im-

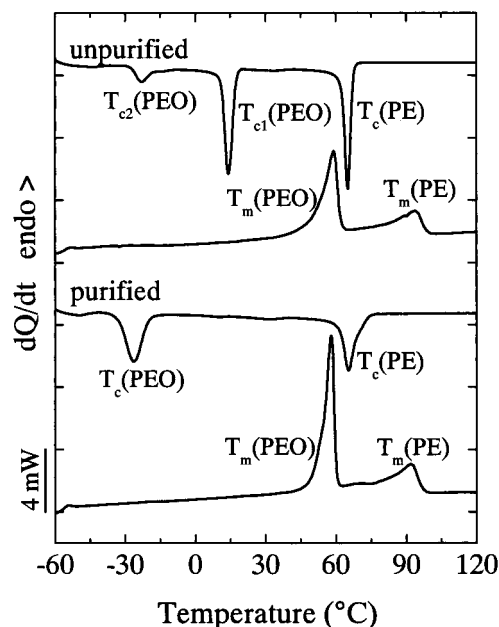


**Figure 2.** Cooling and heating DSC scans of original and purified E24EP57EO1969 triblock copolymer.

**purities.** Chen et al.<sup>22</sup> have claimed that the nucleation events they have observed in confined microdomain structures (MD) within PEO-*b*-PB diblock copolymers must be homogeneous since impurities cannot be contained within the nanoscopic MD they produced. However, we have observed heterogeneous nucleation within confined nanoscopic microdomain structures of crystallizable blocks within ABC triblocks, and an example is presented below.

Figure 2 shows a remarkable example of fractionated crystallization of a PEO block within a PE-*b*-PEP-*b*-PEO triblock copolymer (PEP = poly(ethylene-*alt*-propylene)). The anionically polymerized  $B_{24}I_{56}EO_{20}^{67}$  triblock copolymer was hydrogenated using Wilkinson catalyst in order to produce the  $E_{24}EP_{57}EO_{19}^{69}$ , so in this case the PE block contains ethyl branches from the 1,2 units present in the PB block. Hydrogenation causes a small change in the composition and molecular weight of the copolymer as reflected by the changes in subscripts and superscripts in this case; however, as seen in Table 1, we have used the same subscripts and superscripts for the series of SBC and their hydrogenated counterpart SEC block copolymers presented below to make reading easier.

The cooling scan of the original  $E_{24}EP_{57}EO_{19}^{69}$  sample in Figure 2 shows how, upon cooling from the melt, the PE block crystallizes first. Then, as the temperature is decreased, a large part of the PEO block crystallizes just below  $20$  °C while a small fraction of the PEO can only crystallize at much lower temperatures ( $-20$  °C and below). Such a fractionated crystallization process closely resembles that produced in polymer blends, where the PEO is dispersed into droplets in an immiscible matrix.<sup>1</sup> In this case the PEO is probably confined into either cylinders or spheres, even so the crystallization observed at around  $20$  °C must be due to the presence of heterogeneities in the polymer.

As a matter of fact, since the sample contained the Wilkinson catalyst used for hydrogenation, it was submitted to a purification procedure by which the sample was refluxed in a toluene solution with concentrated HCl and the catalyst was successfully removed.

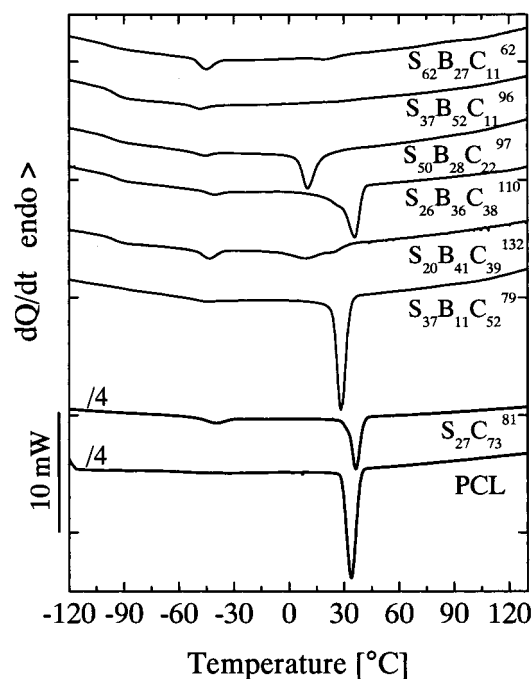


**Figure 3.** Cooling DSC scans (10 °C/min) of a PCL homopolymer, a PS-*b*-PCL diblock copolymer, and PS-*b*-PB-*b*-PCL triblock copolymers.

Figure 2 also shows how the E<sub>24</sub>EP<sub>57</sub>EO<sub>19</sub><sup>69</sup> sample behaves upon cooling from the melt after purification. The exotherm that was present around room temperature has completely disappeared, and all of the PEO is now crystallizing at temperatures lower than -27 °C. In fact, two low crystallization exotherms for the PEO block were identified: one that peaks at around -27 °C and a very small exotherm at -47 °C. The exotherm at -27 °C can be interpreted as the crystallization of the PEO block after heterogeneous nucleation from a weakly nucleating heterogeneity or surface nucleation, and the lowest crystallization exotherm is undoubtedly originated by crystallization after homogeneous nucleation of the PEO block. Table 1 shows that a very similar copolymer that was prepared, E<sub>11</sub>EP<sub>71</sub>EO<sub>18</sub><sup>124</sup>, yielded almost identical results.

**General Fractionated Crystallization Behavior of AB and ABC Triblock Copolymers with Crystallizable Blocks of PCL, PE, or PEO.** Table 1 lists peak crystallization temperatures during cooling DSC scans performed at 10 °C/min for a series of AB and ABC triblock copolymers and selected homopolymers. On the left-hand side of the table, after the homopolymers, data for a series of triblock copolymers incorporating PEO blocks are presented. These data clearly indicate that the PEO exhibits fractionated crystallization when it constitutes a minor component of the block copolymer. In these cases a crystallization peak labeled *T<sub>c</sub>* (II) in Table 1 is exhibited at temperatures below -20 °C. The temperature corresponding to the maximum attainable supercooling is that shown by the S<sub>81</sub>EO<sub>19</sub><sup>18,5</sup> diblock copolymer (i.e., -40 °C peak temperature; Figure 1 shows that the exotherm ends at around -50 °C) and probably represents the crystallization from homogeneous nuclei since the *T<sub>g</sub>* of the PEO block was found in similar materials at -58 °C. Previous reports of similar lower crystallization temperatures can be found in the literature.<sup>20–22</sup> Therefore, the crystallization exotherms of the rest of the PEO copolymers exhibiting crystallization temperatures around -25 °C

may be attributed either to a weak nucleating influence of the interphase or to the existence of other types of heterogeneities that are active at such large undercoolings; see more on this subject below in the self-nucleation section.

Figure 3 shows a series of cooling DSC scans of a PS-*b*-PCL diblock and several PS-*b*-PB-*b*-PCL triblock copolymers where the only crystallizable block is PCL, a PCL homopolymer is also included for comparison purposes. Transmission electron microscopy (TEM) observations after annealing in the melt at 140 °C for several hours (usually 4 h in order to approximate as much as possible to equilibrium morphologies) indicated that the PCL block can be either the matrix or can be confined in lamellae or cylinders.<sup>34</sup> Table 2 summarizes the TEM observations for annealed versions of the samples presented in Figure 3.

It is somewhat unexpected that, for copolymers where PCL is an excess component, fractionated crystallization is still observed, as shown in Figure 3 for S<sub>37</sub>B<sub>11</sub>C<sub>52</sub><sup>79</sup> or S<sub>27</sub>C<sub>73</sub><sup>81</sup>. Nevertheless, the fraction that is crystallizing at lower temperatures is very small as judged by its relative area compared with most of the PCL that is crystallizing after heterogeneous nucleation at around 30 °C (see Table 1). The samples whose DSC scans are presented in Figure 3 were not submitted to special annealing treatment apart from heating them to 140 °C in order to erase thermal history for 3 min. Therefore, their morphologies are probably not as well ordered as those observed with TEM; this may account for the fractionated crystallization being observed in all the samples of Figure 3.<sup>36,37</sup> In the case of the S<sub>37</sub>B<sub>11</sub>C<sub>52</sub><sup>79</sup> triblock copolymer, Table 2 indicates that PCL forms lamellae. If the morphology would be perfectly ordered and no connection between different PCL lamellar microdomain existed, then fractionated crystallization would still be expected. If the morphology is not well ordered and defects cause percolation of the PCL MD, then heterogeneous nucleation can dominate as indicated in Figure 3 for this copolymer. Similar results have been obtained in a recent publication by Loo et al.<sup>37</sup>

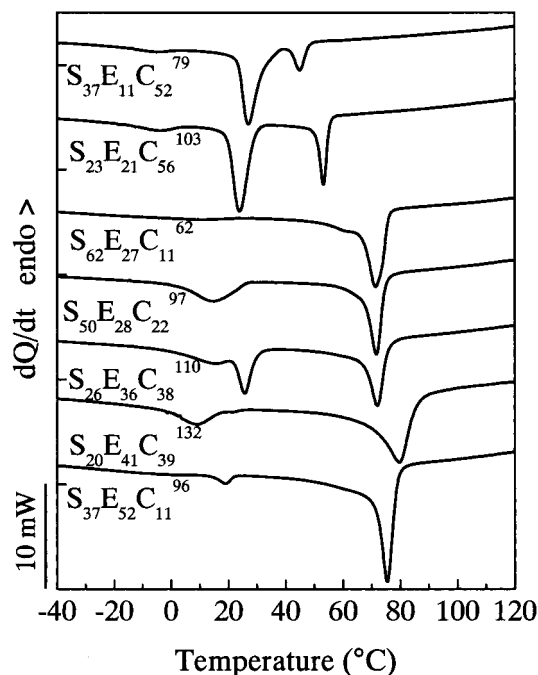
It is noteworthy that when PCL is confined into cylinders in SBC triblock copolymers with only 11% PCL, almost all of their crystallization occurs at temperatures between -45 and -50 °C (see Tables 1 and 2). The glass transition temperature corresponding to the PCL block measured in DSC heating scans for these copolymers was located approximately at -62 °C. Once again, we attribute the low-temperature exotherms observed in Figure 3 at temperatures below -40 °C to the crystallization of PCL block, starting from homogeneous nuclei. This confirms previous findings of Balsamo et al. in SBC and SEC triblock copolymers.<sup>25,26</sup>

The hydrogenated versions of the SBC block copolymers presented above were prepared using Wilkinson catalyst in a similar way to that described in a previous work.<sup>26</sup> Their cooling scans from the melt are presented in Figure 4. The crystallization of the PE block can be observed at temperatures between 90 and 45 °C that depend on the content of ethyl branches present in the chain as indicated in Table 1 and which may also appear at lower temperatures because of fractionated crystallization.

If a comparison is made between all SBC and their SEC counterparts in Table 1 and Figure 4, one common feature that can be observed is the disappearance of

**Table 2. Representative Morphology of Selected Copolymers Observed by TEM after Annealing in the Melt below the Order–Disorder Transition**

polymer	morphology	polymer	morphology
S <sub>62</sub> B <sub>27</sub> C <sub>11</sub> <sup>62</sup>	core–shell-like cylinders with PCL cores	S <sub>26</sub> E <sub>36</sub> C <sub>38</sub> <sup>110</sup>	lamellar–lamellar
S <sub>62</sub> E <sub>27</sub> C <sub>11</sub> <sup>62</sup>		S <sub>20</sub> B <sub>41</sub> C <sub>39</sub> <sup>132</sup>	lamellar–lamellar
S <sub>37</sub> B <sub>52</sub> C <sub>11</sub> <sup>96</sup>	core–shell-like cylinders with PCL cores	S <sub>20</sub> E <sub>41</sub> C <sub>39</sub> <sup>132</sup>	PS cylinders
S <sub>37</sub> E <sub>52</sub> C <sub>11</sub> <sup>96</sup>	PS cylinders	S <sub>37</sub> B <sub>11</sub> C <sub>52</sub> <sup>79</sup>	lamellar–cylindrical with PB cylinders
S <sub>50</sub> B <sub>28</sub> C <sub>22</sub> <sup>97</sup>	core–shell cylinders with PCL cores	S <sub>37</sub> E <sub>11</sub> C <sub>52</sub> <sup>79</sup>	PCL matrix, PE-rings and PS cylinders
S <sub>50</sub> E <sub>28</sub> C <sub>22</sub> <sup>97</sup>	undulated lamellae	S <sub>23</sub> B <sub>21</sub> C <sub>56</sub> <sup>103</sup>	lamellar–lamellar
S <sub>26</sub> B <sub>36</sub> C <sub>38</sub> <sup>110</sup>	lamellar–lamellar	S <sub>23</sub> E <sub>21</sub> C <sub>56</sub> <sup>103</sup>	lamellar–lamellar

**Figure 4.** Cooling DSC scans (10 °C/min) of PS-*b*-PE-*b*-PCL triblock copolymers.

crystallization exotherms at around  $-40$  °C in all SEC polymers. This may be due to the nucleating influence exerted by the Wilkinson catalyst on the PCL block of all the prepared copolymers. Fractionated crystallization of the PCL copolymer still remains in some samples, like in S<sub>23</sub>E<sub>21</sub>C<sub>56</sub><sup>103</sup>, where the PCL block crystallizes principally at around  $24$  °C, but a small exothermic peak can be seen at  $-3$  °C. Nevertheless, the process of homogeneous nucleation of the PCL block is absent in these SEC copolymers.

With regards to the crystallization of the PE block within SEC block copolymers, it is very difficult to ascertain whether homogeneous nucleation is taking place in some copolymers in view of the varying content of ethyl branches. Nevertheless, according to the trend exhibited by the peak crystallization temperature of the PE block within SEC copolymers in Figure 4 and Table 1, it can be seen that copolymers with varying ethyl branching content from 2.6 to 4.1 mol % exhibit crystallization temperatures between  $80$  and  $71$  °C. These temperatures must be characteristic of previous heterogeneous nucleation since the hydrogenated PB reported in Table 1 crystallizes at  $73.4$  °C.

The PE block within S<sub>23</sub>E<sub>21</sub>C<sub>56</sub><sup>103</sup> crystallizes at  $53.3$  °C, and it contains 4.4 mol % ethyl branches. The difference of 0.3 mol % in branch content between S<sub>23</sub>E<sub>21</sub>C<sub>56</sub><sup>103</sup> and S<sub>37</sub>E<sub>52</sub>C<sub>11</sub><sup>96</sup> that crystallizes at  $75.4$  °C (and contains 4.1 mol % of ethyl branches; see Table 1) does not seem to be enough to justify a depression of  $T_c$  of  $22$  °C. For example, the use of Flory's equation<sup>37</sup> to

predict the melting point depression in random copolymers would yield a difference in melting temperatures of only  $5$  °C for this difference in branch content. However, it must be remembered that usually differences in  $T_c$  are expected to be higher so this argument has to be used with caution.<sup>38</sup> It is therefore plausible that in the case of the S<sub>23</sub>E<sub>21</sub>C<sub>56</sub><sup>103</sup> copolymer the PE block may be crystallizing exclusively from less active heterogeneities than usual or from homogeneous nuclei. Other SEC copolymers exhibit some crystallization in the temperature range between  $55$  and  $45$  °C and may therefore be also showing some crystallization from homogeneous nuclei or fractionated crystallization (see for instance S<sub>62</sub>E<sub>27</sub>C<sub>11</sub><sup>96</sup> in Figure 4). We had previously found crystallization of the PE block within SEC copolymers at similar low-temperature regions<sup>39</sup> but did not ascribe them to fractionated crystallization processes in view of the uncertainty that arises with the crystallization temperature dependence on ethyl branching content. However, in the light of the recent publication of Loo et al.<sup>15</sup> and the data presented in this work, it is possible that the low-temperature crystallization exotherms encountered when the PE block was confined, as in the copolymers S<sub>35</sub>E<sub>15</sub>C<sub>50</sub><sup>150</sup> and S<sub>27</sub>E<sub>15</sub>C<sub>58</sub><sup>219</sup> in ref 39, were due to fractionated crystallization or even homogeneous nucleation. (The peak crystallization temperatures of the PE block upon cooling from the melt at  $10$  °C/min was  $61.5$  °C for S<sub>35</sub>E<sub>15</sub>C<sub>50</sub><sup>150</sup>.)

The above results show that, like in the case of polymer blends,<sup>1,2</sup> it is a consequence of confinement, i.e., the lack of a high enough number of heterogeneities, what is causing the homogeneous nucleation in crystallizable blocks when they are in MD-like cylinders or spheres regardless of the specific shape of the isolated MD. This can be demonstrated by finding a way to inject heterogeneities into the confined microphase-separated polymer. In the case of polymer blends this has been easily achieved by the addition of suitable nucleating agents,<sup>2,16–18</sup> and in the case of block copolymers we have provided examples like the Wilkinson catalyst above. Another way to inject very effective nuclei is by self-nucleating the confined crystallizable polymer,<sup>2,16–19,28,39</sup> since its own crystals should provide ideal surfaces for epitaxial nucleation.

**Self-Nucleation Behavior of Crystallizable Blocks within AB and ABC Block Copolymers.** Figure 5a shows cooling DSC scans from the indicated  $T_s$  temperatures for a S<sub>27</sub>C<sub>73</sub><sup>81</sup> diblock copolymer. In view of its composition, the PCL block is probably the matrix component (unless it is forming lamellae, which could also be possible). Nevertheless, a very small fraction of material is crystallizing at  $-39$  °C, while the majority of the material exhibits a crystallization exotherm at  $36.5$  °C (see the curve corresponding to  $T_s = 140$  °C in Figure 5a).

The self-nucleation domain or domain II starts at  $T_s = 64$  °C in Figure 5a for the S<sub>27</sub>C<sub>73</sub><sup>81</sup> diblock copolymer,



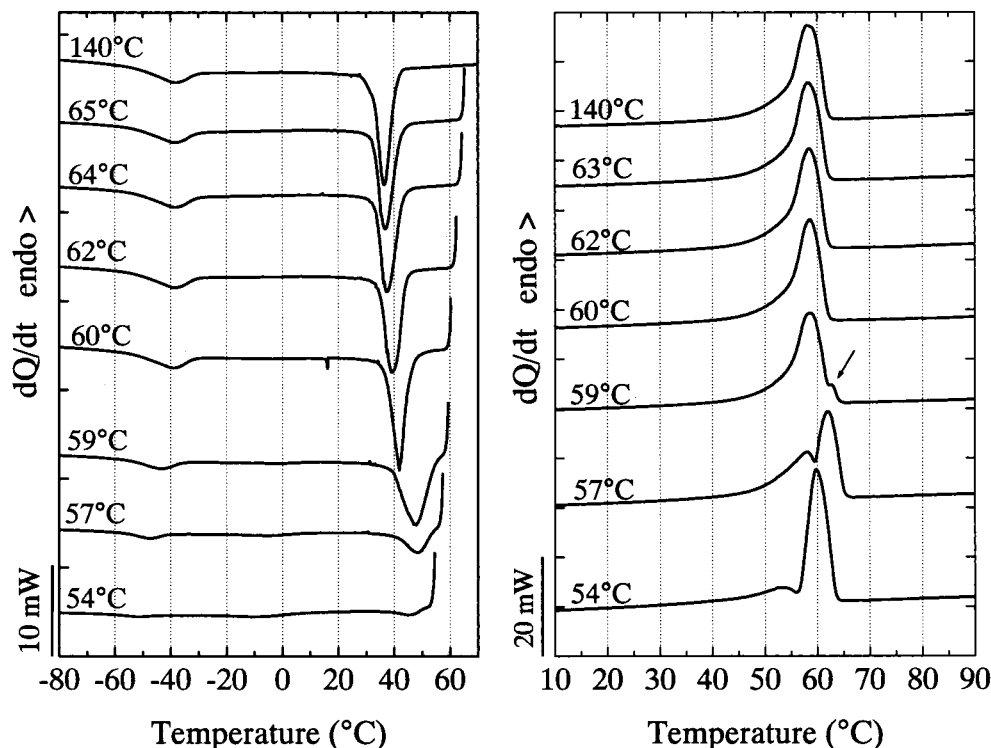


**Figure 5.** (a) Cooling DSC scans (10 °C/min) from the indicated  $T_s$  temperatures for a  $S_{27}C_{73}$  diblock copolymer. (b) Subsequent heating DSC scans (10 °C/min) after self-nucleation at the indicated temperatures.

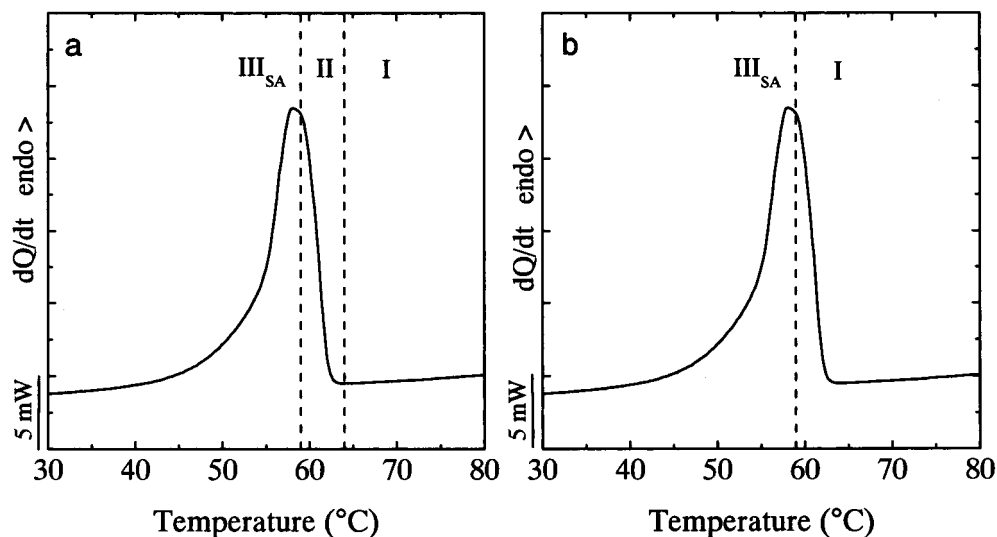


**Figure 6.** Self-nucleation domains for a  $S_{27}C_{73}$  diblock copolymer. Self-nucleation behavior of the material that crystallizes in (a) exotherm I and (b) exotherm II (see Table 1 and text).

where a small increase in the peak crystallization temperature of signal I or high-temperature crystallizing signal (this nomenclature is consistent with Table 1) can be observed upon cooling. Lower  $T_s$  temperatures cause bigger displacements in  $T_c$  (I) until  $T_s = 59$  °C, where the crystallization seems to start right from the beginning of the cooling run. This usually means that self-nucleation and annealing are simultaneously present.<sup>28,33,39</sup> This can be corroborated in the subsequent heating run presented in Figure 5b for the same  $T_s = 59$  °C, where a small high-temperature melting peak appears, and it is indicated with an arrow for the heating scan after heat treatment at 59 °C. From this  $T_s$  temperature downward, domain III has been reached. Further decreases in  $T_s$  mean that the amount of unmelted material at  $T_s$  is higher and so is the number

of annealed crystals as indicated by the increase in size of the higher melting temperature endotherm, which also moves to lower values as  $T_s$  is decreased (see curves corresponding to  $T_s$  temperatures of 59, 57, and 54 °C in Figure 5b). The crystals that formed in exotherm I in Figure 5a (i.e., whose  $T_c$  (I) is 36.5 °C at  $T_s = 140$  °C) can be self-nucleated and annealed and follow the expected behavior of a regular bulk crystallizable polymer.<sup>28,33,39</sup> The classical self-nucleation domains are drawn on the original melting trace of the copolymer in Figure 6a where the usual depiction of the three self-nucleation domains can be observed.<sup>33</sup>

On the other hand, the crystal population labeled II in Table 1 for this  $S_{27}C_{73}$  copolymer does not behave in a common way with respect to self-nucleation. Figure 5a,b shows that this crystal population does not experi-

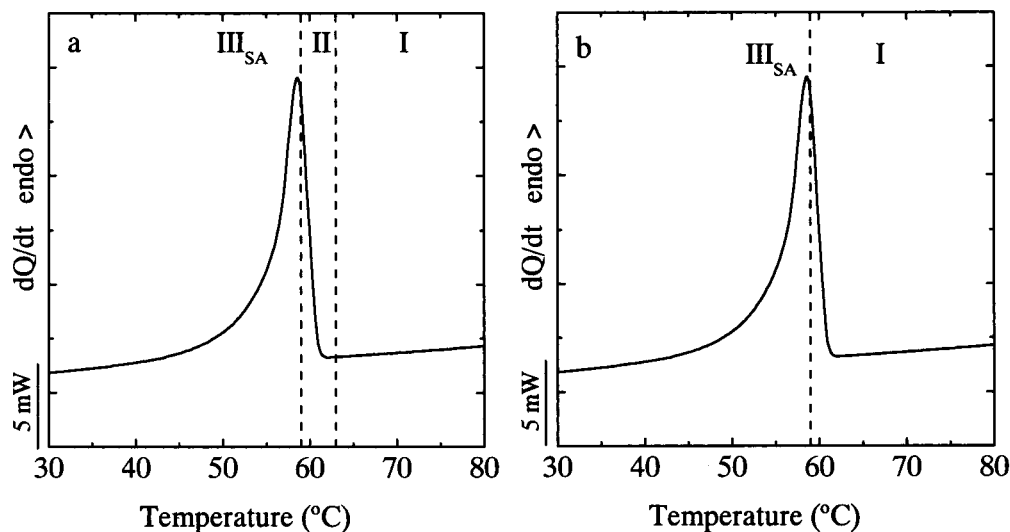


**Figure 7.** Self-nucleation domains for a  $S_{26}B_{36}C_{38}^{110}$  triblock copolymer. Self-nucleation behavior of the material that crystallizes in (a) exotherm I and (b) exotherm II (see Table 1 and text).

ence any change until at a  $T_s = 59^\circ\text{C}$  it starts to respond by self-nucleation, once annealed crystals are present. Only part of the original exotherm II is self-nucleated and crystallizes with the rest of the PCL at temperatures higher than  $40^\circ\text{C}$ , while the rest that is left to crystallize from homogeneous nuclei shows a  $T_c$  at around  $-45^\circ\text{C}$ . This behavior is analogous to that exhibited by a PE block within a  $S_{35}E_{15}C_{50}^{150}$  block copolymer.<sup>39</sup> It seems that in this case domain II has completely disappeared as denoted in Figure 6b; see below for more details on this effect.

The self-nucleation behavior of the PCL block within a  $S_{26}B_{36}C_{38}^{110}$  triblock copolymer that displays a lamellar morphology (see Table 2) is summarized in Figure 7. It basically follows an identical behavior to that of the diblock copolymer presented in Figures 5 and 6. Here, the fraction of crystals formed at higher temperatures (at  $T_c$  (I), Table 1) exhibit again the three classical nucleation domains schematically indicated in Figure 7a. On the other hand, those crystals that were homogeneously nucleated (i.e., those that crystallized at  $T_c$  (II), Table 1) can only be self-nucleated at  $T_s$  temperatures where domain III has already started; therefore, domain II disappears as shown in Figure 7b.

The triblock copolymer  $S_{62}B_{27}C_{11}^{62}$  is very interesting because it exhibits a peculiar morphology. Figure 8 shows a TEM micrograph of an annealed ultrathin section of this copolymer that has been stained by  $\text{OsO}_4$  inducing a black color on the PB phase, a gray tone on the PS phase, and no color (white) on the unstained PCL phase. It must be noted that this sample does not have a well-developed long-range order. Nevertheless, on the basis of the spherical features and on the parallel lines on the image, one can assume B-shells around C-cores in an A matrix as indicated in the small schematic drawing in Figure 8. Then, the PCL block is confined in cylinders within  $S_{62}B_{27}C_{11}^{62}$ , and its DSC cooling scan, displayed in Figure 9a, shows almost exclusive crystallization at  $-45^\circ\text{C}$  and just a trace of crystallization at around  $20^\circ\text{C}$  that is very difficult to appreciate in view of the scale.

The almost exclusive homogeneous nucleation of the PCL chains within cylinders in  $S_{62}B_{27}C_{11}^{96}$  is clearly due to the vast number of cylinders as compared to heterogeneous nuclei. The number of cylinders can be roughly

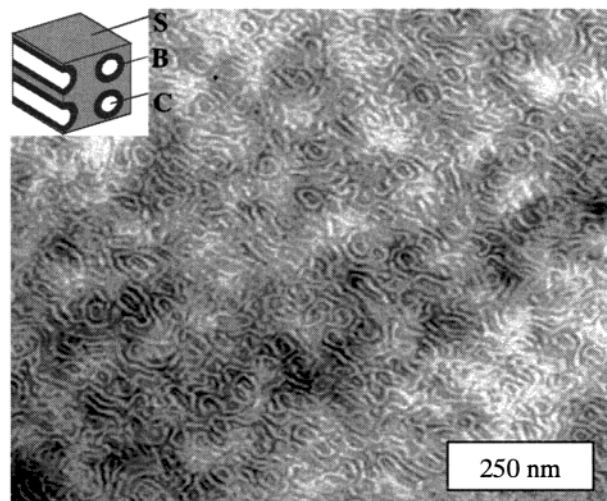


**Figure 8.** TEM micrograph of  $S_{62}B_{27}C_{11}^{96}$ .

estimated from Figure 8 and the section thickness, and it is on the order of  $6 \times 10^{15}$  cylinders/ $\text{cm}^3$ , while the heterogeneity density in PCL is around  $10^7$  particles/ $\text{cm}^3$  according to experiments performed by counting nascent spherulites in thin films under the optical microscope.

The self-nucleation of this homogeneously nucleated PCL block confined in core-shell like cylinders within a PS matrix (Figure 8) confirms the observed behavior described above for all the crystal PCL population that was nucleated homogeneously. To be able to self-nucleate these chains within PCL cylinders that would normally nucleate homogeneously, it is important to leave a great number of crystal fragments. As a matter of fact, the subsequent heating traces, not shown here, revealed that annealing started at  $T_s = 59^\circ\text{C}$ . However, the amount of annealed crystals and self-nuclei was not enough to initiate the self-nucleation process. Therefore, a transition from domain I to domain III<sub>A</sub> (the A stands for annealing without self-nucleation) was detected. A similar result was obtained when the self-nucleation domains were studied in highly confined PE blocks within  $S_{35}E_{15}C_{50}^{150}$  and  $S_{27}E_{15}C_{58}^{219}$  (see ref 39).

Only when there are enough self-nuclei at  $T_s = 57^\circ\text{C}$  was self-nucleation of the PCL block detected for



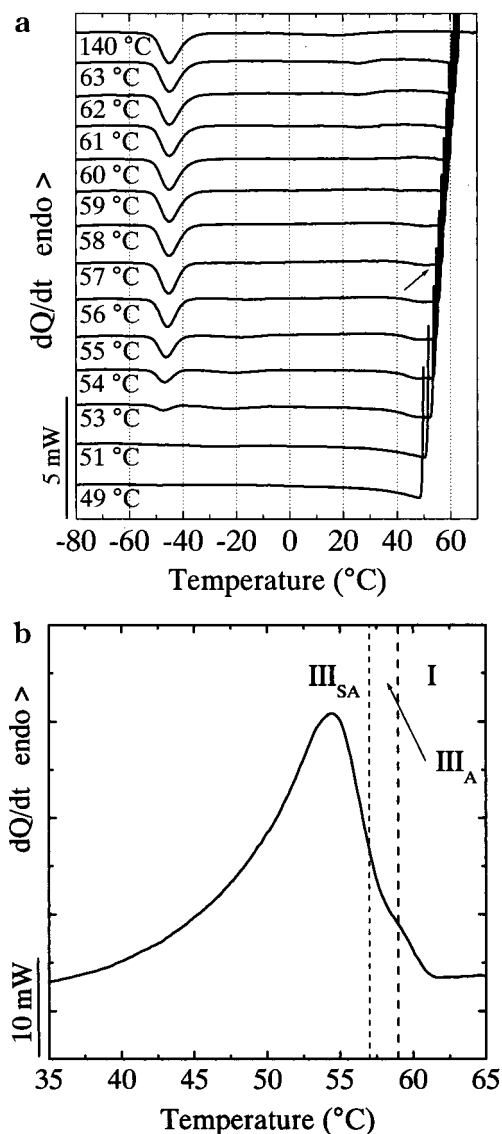


**Figure 9.** (a) Cooling DSC scans (10 °C/min) from the indicated  $T_s$  temperatures for a  $S_{62}B_{27}C_{11}$  triblock copolymer. (b) Self-nucleation domains for  $S_{62}B_{27}C_{11}$ .

$S_{62}B_{27}C_{11}$ <sup>96</sup>, as indicated in Figure 9a by the rather small exotherm that appears just upon cooling from  $T_s$  at high temperatures (see arrow in Figure 9a). Domain  $III_{SA}$  had been attained at this  $T_s$ , a fact depicted in Figure 9b. The low-temperature exotherm in Figure 9a is seen to be progressively reduced in size as  $T_s$  is decreased, while the crystallization at temperatures above 40 °C is more apparent. The small remaining molten fraction of PCL is completely self-nucleated by annealed crystals at  $T_s$  lower than 53 °C. Therefore, upon cooling from temperatures lower than 53 °C, crystallization only occurs immediately upon cooling (i.e., a small exotherm can be observed in Figure 9a, curve corresponding to  $T_s = 49$  °C, at the beginning of the cooling run that extends down to 40 °C while the exotherm at -45 °C disappeared completely).

The results presented above on the self-nucleation behavior of the PCL within PS-*b*-PCL and PS-*b*-PB-*b*-PCL copolymers seem to be a general trend in AB and ABC block copolymers. Heterogeneity free MD will nucleate homogeneously as expected. However, domain II is absent or not observed. This is a result of the great number of self-seeds that these crystallizable blocks

demand in order to be self-nucleated since they are confined into MD-like cylinders or spheres where the density of such regions can be as high as  $10^{15}$ – $10^{16}/\text{cm}^3$ . This means that the number of cylinders exceeds the number of active heterogeneities by several orders of magnitude (i.e., as high as 8 or 9 orders of magnitude in the PCL case).

It is well-known that as  $T_s$  decreases, the nucleation density sharply increases as self-nuclei are produced in the material.<sup>33</sup> In the case of crystallizable blocks within the confined MD,  $T_s$  needs to be lowered to such an extent that partial melting occurs extensively, and annealing is produced even before self-nucleation in every MD can be realized.

The PEO block, when it is confined in cylinders or spheres in  $S_{81}EO_{19}$ <sup>18,5</sup> or in  $S_{63}EO_{16}C_{21}$ <sup>24</sup>, also exhibited a very similar behavior to that described above for the PCL block within SBC or SC block copolymers.<sup>28</sup> However, in the triblock copolymer we observed coincident homogeneous nucleation and subsequent crystallization of both the PEO and the PCL blocks, since they both crystallize; see refs 27 and 29.

Figure 10 shows the self-nucleation behavior of the PEO block within the purified triblock copolymer  $E_{24}EP_{37}EO_{19}$ <sup>69</sup>. Only the region where the PEO is being self-nucleated is presented in Figure 10a. As indicated in Figure 2, after purification, only the low-temperature crystallization of the PEO block remained. As pointed out above, the crystallization at -27 °C is probably due to crystallization after some weak nucleating effect of either the interphase or some less efficient type of heterogeneity. Even so, it also exhibits the self-nucleation behavior shown above for heterogeneity free PCL or PEO chains within cylinders. Figure 10b shows that domain II is absent, and self-nucleation clearly starts at  $T_s = 56$  °C, when annealed crystals are already present. Figure 10a shows in this case even more clearly than other examples presented above, how when part of the PEO chains are being self-nucleated, the crystallization is fractionated and occurs in two steps (see arrows). The first part crystallizes just upon cooling from  $T_s$ , see the curve corresponding to  $T_s = 56$  °C, in a temperature range spanning from  $T_s$  down to 40 °C, while the rest crystallizes in the original low-temperature range from -20 to -35 °C. On the other hand, the small exotherm at -55 °C is still present after self-nucleation at  $T_s = 50$  °C, indicating that even lower  $T_s$  temperatures would be required to self-nucleate such small population of homogeneously nucleated crystals.

If the PEO block in the unpurified version of  $E_{24}EP_{57}EO_{19}$ <sup>69</sup> (shown in Figure 2) is self-nucleated, it behaved just like the PCL block in  $S_{26}B_{36}C_{38}$ <sup>110</sup> with a behavior that *mutatis mutandis* mimics the one shown in Figure 7. In view of the self-nucleation results for  $E_{24}EP_{57}EO_{19}$ <sup>69</sup>, it seems more likely that the reason behind the low-temperature crystallization for the PEO block is a weak nucleation effect of the interphase rather than the presence of heterogeneities with low nucleation efficiency, but it is still difficult to ascertain this fact.

In a previous work,<sup>39</sup> the self-nucleation of the PE central block within a series of PS-*b*-PE-*b*-PCL triblock copolymers was studied. It was found that, as the amount of the PE block within the copolymers was reduced, the self-nucleation behavior changed from the classical three domain to one where domain II was absent, and the chains experienced a similar situation to that shown in Figure 8 for the PCL block: transitions

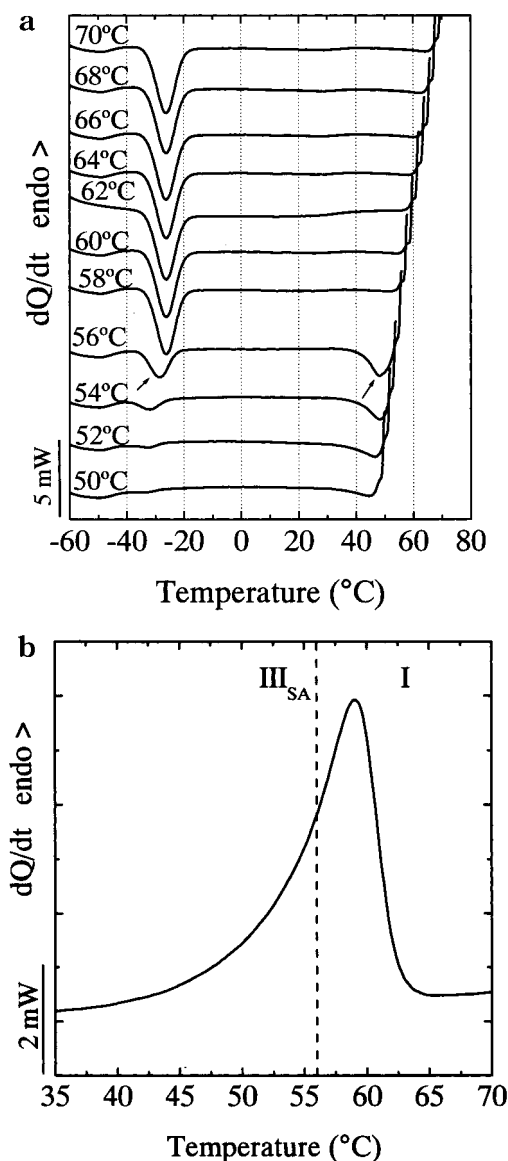


**Figure 10.** (a) Cooling DSC scans (10 °C/min) from the indicated  $T_s$  temperatures for purified  $E_{24}EP_{37}EO_{19}$ <sup>69</sup> triblock copolymer. (b) Self-nucleation domains for purified  $E_{24}EP_{37}EO_{19}$ <sup>69</sup>.

from domain I to  $III_A$  and finally to  $III_{SA}$  as  $T_s$  was reduced. An example of such behavior is provided in Figure 11 for  $S_{27}E_{15}C_{58}$ <sup>219</sup>. It is interesting to note that this copolymer contains 2.6 mol % ethyl branches or the same amount than that in the hydrogenated polybutadiene presented as PE in Table 1 with a  $T_c$  of 73.5 °C. Nevertheless, as indicated in Figure 11a, the PE block within  $S_{27}E_{15}C_{58}$ <sup>219</sup> crystallizes at 61 °C with an increase in supercooling of 12.5 °C.<sup>39</sup> This could be interpreted as fractionated crystallization that may have originated in homogeneous nuclei. The self-nucleation domains for the PE block within this copolymer are presented in Figure 11b and follow the pattern shown above for highly confined PCL and PEO blocks that nucleate homogeneously, i.e., absence of domain II and in this case a split of domain III in  $III_A$  and  $III_{SA}$ .

## Conclusions

The study of nucleation and crystallization of confined PEO, PCL, and PE blocks within a wide range of AB and ABC block copolymers has shown that fractionated

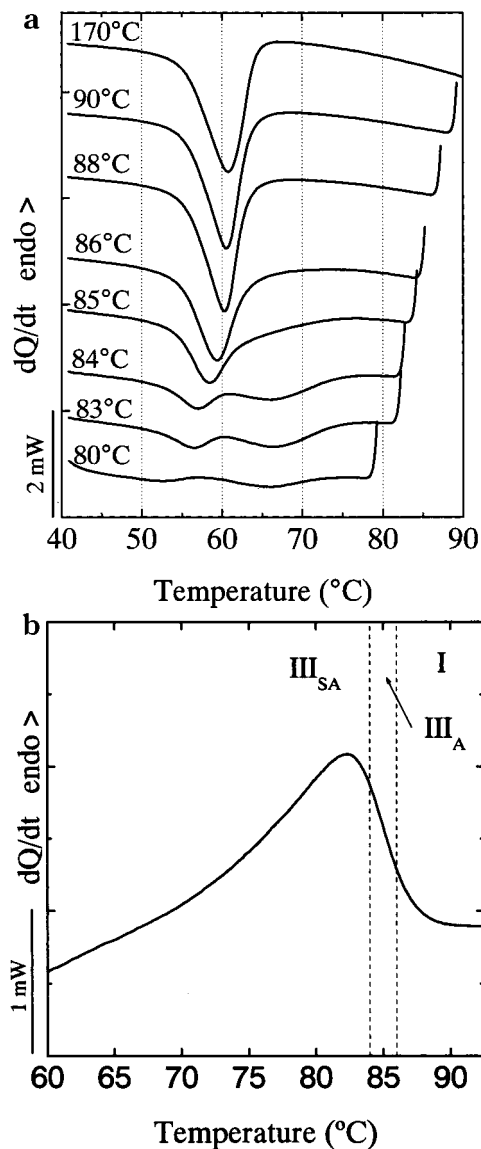


**Figure 11.** (a) Cooling DSC scans (10 °C/min) from the indicated  $T_s$  temperatures for a  $S_{27}E_{15}C_{58}$ <sup>219</sup> triblock copolymer. (b) Self-nucleation domains for  $S_{27}E_{15}C_{58}$ <sup>219</sup>.

crystallization can developed in a way that resembles crystallization in isolated microphases within immiscible polymer blends. The density of confined microdomain structures (MD) in the block copolymer cases is much higher than the number of heterogeneities available in each crystallizable block. Then, fractionated crystallization takes place with one or several crystallization steps at decreasing temperatures. In specific cases, the clear observation of exclusive crystallization from homogeneous nuclei was obtained.

The results have demonstrated that it is the lack of a high enough number of heterogeneities that is causing the homogeneous nucleation in crystallizable blocks within block copolymers when they are in isolated MD like cylinders or spheres, regardless of their shape.

Contrary to what is found in polyblends, the crystal population that arises from homogeneous nuclei or others at very low temperatures cannot be nucleated by the self-seeding nuclei produced in domain II; therefore, domain II disappears. Self-nucleation only takes place when  $T_s$  is lowered well into domain III since a higher density of self-nuclei is needed in order to

nucleate highly confined block copolymer components. In this last case, some copolymers required even lower self-nucleation temperatures than usual; in such cases domain III was found to split in a pure annealing domain (i.e., domain III<sub>A</sub>) and a self-nucleation and annealing domain at lower  $T_s$  temperatures (i.e., domain III<sub>SA</sub> or the usual domain III). This is a direct consequence of the extremely high density of MD that need to be self-seeded when crystallizable blocks are confined in spheres or cylinders depending on composition (on the order of  $10^{15}$ – $10^{16}$ /cm<sup>3</sup>). Therefore, to increase the density of self-nuclei to comparable values, the self-nucleation temperature  $T_s$  has to be decreased to values so low that partial melting is achieved, and some of the unmelted crystal fragments can be annealed, sometimes even before self-nucleation takes place.

**Acknowledgment.** This work was made possible by the financial support of CONICIT through Grant G97-000594, by DSM, and by the European Union (Alfa exchange program). Helpful discussions with Dr. G. Reiter and early disclosure of his unpublished results are also acknowledged.

## References and Notes

- (1) Frensch, H.; Harnischfeger, P.; Jungnickel, B.-J. Fractionated Crystallization in Incompatible Polymer Blends. In *Multiphase Polymers: Blends and Ionomers*; Utracky, L. A., Weiss, R. A., Eds.; ACS Symp. Ser. **1989**, 395, 101.
- (2) Arnal, M. L.; Matos, M. E.; Morales, R. A.; Santana, O. O.; Müller, A. J. *Macromol. Chem. Phys.* **1998**, 199, 2275.
- (3) Zettlemoyer, A. C., Ed.; *Nucleation*; Marcel Dekker: New York, 1969.
- (4) Vonnegut, B. J. *Colloid Sci.* **1948**, 3, 563.
- (5) Turnbull, D.; Cech, R. E. *J. Appl. Phys.* **1950**, 21, 804.
- (6) Pound, G. M.; La Mer, V. K. *J. Am. Chem. Soc.* **1952**, 74, 2323.
- (7) Turnbull, D. *J. Chem. Phys.* **1952**, 20, 411.
- (8) Turnbull, D.; Cormia, R. L. *J. Chem. Phys.* **1961**, 34, 820.
- (9) Cormia, R. L.; Price, F. P.; Turnbull, D. *J. Chem. Phys.* **1962**, 37, 1333.
- (10) Burns, J. R.; Turnbull, D. *J. Appl. Phys.* **1966**, 37, 4021.
- (11) Koutsky, J. A.; Walton, A. G.; Baer, E. *J. Appl. Phys.* **1967**, 38, 1832.
- (12) Gornick, F.; Ross, G. S.; Frolen, L. J. *J. Polym. Sci., Part C* **1967**, 18, 79.
- (13) Barham, P. J.; Jarvis, D. A.; Keller, A. *J. Polym. Sci., Polym. Phys. Ed.* **1982**, 20, 1733.
- (14) Arnal, M. L.; Müller, A. J. *Macromol. Chem. Phys.* **1999**, 200, 2559.
- (15) Loo, Y.; Register, R.; Ryan, A. J. *Phys. Rev. Lett.* **2000**, 84, 4120.
- (16) Santana, O. O.; Müller, A. J. *Polym. Bull. (Berlin)* **1994**, 32, 471.
- (17) Manaure, A. C.; Morales, R. A.; Sánchez, J. J.; Müller, A. J. *J. Appl. Polym. Sci.* **1997**, 66, 2481.
- (18) Manaure, A.; Müller, A. J. *Macromol. Chem. Phys.* **2000**, 201, 958.
- (19) Arnal, M. L.; Müller, A. J.; Maiti, P.; Hikosaka, M. *Macromol. Chem. Phys.* **2000**, 201, 2493.
- (20) Lotz, B.; Kovacs, A. J. *Polym. Prepr. (Am. Chem. Soc., Div. Polym. Chem.)* **1969**, 10, 820.
- (21) Robitaille, C.; Prud'homme, J. *Macromolecules* **1983**, 16, 665.
- (22) Chen, H.; Hsiao, S.; Lin, T.; Yamauchi, K.; Hasegawa, H.; Hashimoto, T. *Macromolecules* **2001**, 34, 671. Chen, H.; Wu, J.; Lin, J. *Macromolecules* **2001**, 34, 6936.
- (23) Weimann, P. A.; Hajduk, D. A.; Chu, C.; Chaffin, K. A.; Brodil, J. C.; Bates, F. S. *J. Polym. Sci., Part B: Polym. Phys.* **1999**, 37, 2053.
- (24) Reiter, G.; Castelein, G.; Sommer, J.-U.; Röttele, A.; Thurn-Albrecht, T. *Phys. Rev. Lett.* **2001**, 87, 226101.
- (25) Balsamo, V.; von Gyldenfeldt, F.; Stadler, R. *Macromol. Chem. Phys.* **1996**, 197, 3317.
- (26) Balsamo, V.; Müller, A. J.; von Gyldenfeldt, F.; Stadler, R. *Macromol. Chem. Phys.* **1998**, 199, 1063.
- (27) Arnal, M. L.; Balsamo, V.; López-Carrasquero, F.; Contreras, J.; Carrillo, M.; Schmalz, H.; Abetz, V.; Laredo, E.; Müller, A. J. *Macromolecules* **2001**, 34, 7973.
- (28) Müller, A. J.; Arnal, M. L.; López-Carrasquero, F. *Macromol. Symp.*, in press.
- (29) Arnal, M. L.; López-Carrasquero, F.; Laredo, E.; Müller, A. J. Manuscript in preparation.
- (30) Balsamo, V. Ph.D. Thesis, Mainz University, Germany, 1996.
- (31) Balsamo, V.; von Gyldenfeldt, F.; Stadler, R. *Macromol. Chem. Phys.* **1996**, 197, 3317.
- (32) Jakob, T. Ph.D. Thesis, Bayreuth University, Germany, 2000.
- (33) Fillon, B.; Wittman, J. C.; Lotz, B.; Thierry, A. *J. Polym. Sci., Part B: Polym. Phys.* **1993**, 31, 1383.
- (34) Hamley, I. W. *The Physics of Block Copolymers*; Oxford University Press: Oxford, 1998.
- (35) Huang, P.; Zhu, L.; Cheng, S. Z. D.; Ge, Q.; Quirk, R. P.; Thomas, E. L.; Lotz, B.; Hsiao, B. S.; Liu, L.; Yeh, F. *Macromolecules* **2001**, 34, 6649.
- (36) Balsamo, V.; Gil, G.; Urbina de Navarro, C.; Hamley, I. W.; von Gyldenfeldt, F.; Abetz, V. Manuscript in preparation.
- (37) Loo, Y.-L.; Register, R. A.; Ryan, A. J.; Dee, G. T. *Macromolecules* **2001**, 34, 8968.
- (38) Mandelkern, L. In *Physical Properties of Polymers*, 2nd ed.; American Chemical Society: Washington, DC, 1993; Chapter 4.
- (39) Balsamo, V.; Paolini, Y.; Ronca, G.; Müller, A. J. *Macromol. Chem. Phys.* **2000**, 201, 2711.

MA012026W